Matrix Isolation Fourier Transform Infrared Study of Photodecomposition of Formimidic Acid

Fabrice Duvernay, Aurelien Trivella, Fabien Borget, Stephane Coussan, Jean-Pierre Aycard, and Thierry Chiavassa*

Physique des Interactions Ioniques et Moléculaires, Unité mixte de recherche 6633, Université de Provence et Centre National de la Recherche Scientifique, Centre de St Jérôme, case 252, 13397 Marseille Cedex 20, France

The UV isomerization of formamide ($HCONH_2$) trapped in xenon, nitrogen, argon, and neon cryogenic matrices has been monitored by Fourier transform infrared (FT-IR) spectroscopy. Formamide monomer is the only species present in the matrices after deposition; when UV-selective irradiation was carried out at 240 nm, the $n \rightarrow \pi^*$ transition allowed us to observe the formation of several isomers of formimidic acid [H(OH)C═NH]. On these latter species, we carried out selective IR irradiation of their OH stretching mode and compared the experimental and theoretical (B3LYP/6-311+G(2d,2p)) sets of bands. This study allowed us to characterize for the first time all the isomers of formimidic acid. We have then studied the vacuum UV photodecomposition ($\lambda > 160$ nm) of this molecule at 10 K in argon and xenon matrices. Several primary photoproducts such as $HCN \cdot H_2O$, $HNC \cdot H_2O$, and $HNCO \cdot H_2$ complexes, yielded by dehydration and dehydrogenation processes, were characterized.

1. Introduction

Formamide/formimidic acid, of CH_3NO molecular formula, represents the simplest form of amide/imidic acid tautomerism, which is known to play an important role in many areas of chemistry and biochemistry.[1] Selective UV irradiations at 193 nm of formamide isolated in argon matrix have been performed by Lundell et al.,[2] leading to the characterization of the photoproducts: $CO \cdot NH_3$ and $HNCO \cdot H_2$ complexes.[2] On the other hand, UV irradiation at 248 nm in argon matrix with a KrF excimer laser was performed by Maier and Endres,[3] leading through a 1−3 hydrogen transfer to the formimidic acid (H(OH)C═NH), a tautomer of the formamide. Several cases of UV-induced intramolecular proton-transfer reaction from the NH group of amide or thioamide have been already observed in cryogenic matrix.[4−7] Maier and Endres[3] have shown by comparison between the experimental and calculated IR spectra that formimidic acid is present in argon matrix as two forms called (s-*Z*)-(*E*) and (s-*Z*)-(*Z*) as displayed in Scheme 1. Among the four possible conformers of formimidic acid, the most stable was found to be the (s-*Z*)-(*E*) form, predicted to be 50 kJ mol^{-1} less stable than formamide.[8] However, formimidic acid is found to be more stable than the other CH_3NO isomers such as formaldoxime, nitrosomethane, nitrone, and oxaziridine. The barrier estimated by ab initio calculations in the ground state for the conversion between formamide and formimidic acid is relatively high (200 kJ mol^{-1} above formamide).[8] The energy needed to get over this barrier can be provided by the resonant excitation of the forbidden $n \rightarrow \pi^*$ transition located at 219 nm (ca. 544 kJ mol^{-1}).[9−11]

In this paper we present selective UV irradiation (240 nm) of formamide in different environments (Xe, N_2, Ar, and Ne) leading to the formimidic acid. Then we suggest the vibrational

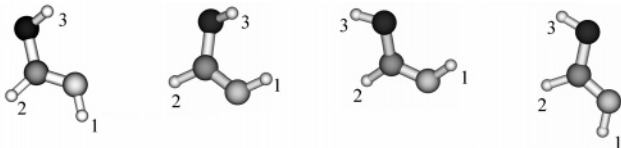**SCHEME 1: Phototautomeric Reaction of Formamide**

(s-*Z*)-(*E*)   (s-*Z*)-(*Z*)
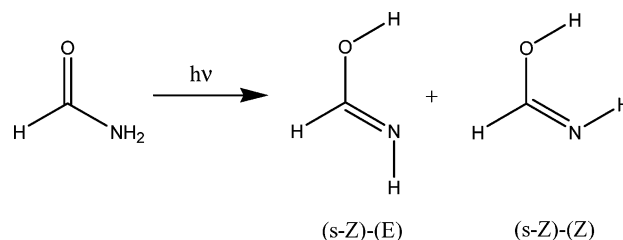
assignments of the different formimidic acid isomers obtained by selective IR irradiation in the ν(OH) region and supported by theoretical calculations. We report the results relative to the photolysis of the formimidic acid that have been performed with broad-band UV irradiation of a H_2 lamp irradiating at $\lambda > 160$ nm. We give evidence of dehydrogenation and dehydration processes that lead to the formation of complexes such as $HNCO \cdot H_2$ and $HCN \cdot H_2O$.

2. Experimental Details

Formamide was obtained from Aldrich (99% purity) and purified under vacuum and prolonged degassing at 50 °C. The vapor pressure of formamide is too low to be handled by the usual vacuum line method. Thus, it is placed into a small glass tube, which is connected to the cryostat and then entrained at room temperature with argon (Linde, 99.99% purity), neon (Air Liquide, 99,99% purity), xenon (Air Liquide, 99.99% purity), or nitrogen, N_2 (Air Liquide, 99.99% purity) on a Au-plated cube of copper cooled between 4 and 10 K. Under these conditions, we cannot determine accurately the formamide concentration in the host gases; we can only state that we worked with a large excess of host gases in the mixture (around 1/500). During the deposition, the cryostat is kept under a limit and constant pressure of 10^{-7} mbar and the sample is deposited at 4, 20, 25, and 30 K in Ne, Ar, N_2, and Xe matrices, respectively.

* Corresponding author: Tel +33 491-288-580; fax +33 491-636-510; e-mail Thierry.chiavassa@up.univ-mrs.fr.

TABLE 1: Theoretical Geometrical Parameters of the Four Stereoisomers of Formimidic Acid[a]

Geometrical parameters	(s-Z)-(E): (1)	(s-Z)-(Z): (2)	(s-E)-(Z): (3)	(s-E)-(E): (4)
r(OH)	0.965	0.965	0.963	0.961
r(CO)	1.346	1.359	1.365	1.355
r(C=N)	1.206	1.259	1.254	1.254
r(NH₁)	1.014	1.02	1.02	1.014
r(CH₂)	1.088	1.085	1.088	1.099
r(OH₃—N)	2.3	2.5	3.1	3.05
(H₃OC)	107.23	109.9	110.2	109.8
(CNH₁)	111.68	113.5	111.6	110.8
(OCN)	122	129.6	124.5	119.8
(H₂COH₃)	180	180	0	0
(H₂CNH₁)	0	180	180	0
E_relative	0	15	15.5	23

[a] Bonds (*r*) are given in angstroms; angles (α) and dihedral angles (γ) are given in degrees. Energies are in kilojoules per mole. Theoretical parameters were obtained by use of B3LYP/6-311+G(2d,2p).

Formimidic acid [H(OH)C=NH] was generated by UV photolysis (240 nm) of formamide (HCONH₂) at 4 K in rare gas matrices (Ar, Ne, and Xe) and in N₂ matrices.

For the irradiation (UV and IR), we used a BMI (Thales Laser) pulsed tunable UV−visible−IR OPO laser (average power: UV, 4 mW; IR, 8 mW). The radiation bandwidth was less than 5 cm⁻¹, the pulse duration was 15 ns, the repetition rate was 10 Hz, and the tuning range was 225−800 nm for UV−visible and 3700−2500 cm⁻¹ for IR. Spectra between 4000 and 500 cm⁻¹ were recorded with a Bruker IFS 66/S spectrometer equipped with a liquid N₂-cooled detector, at a resolution of 0.12 cm⁻¹.

Vacuum UV irradiation (λ > 160 nm) of formimidic acid carried out after laser irradiation at 240 nm was performed on another cryogenic head, equipped with a microwave discharge hydrogen flow lamp (Opthos Instuments) mounted directly onto the sample chamber. The radiations are transmitted to the substrate through a SiO₂ window in a range up to 160 nm. These UV irradiation experiments (λ > 160 nm) were followed by infrared spectroscopy. The spectra were recorded in transmission-reflection mode between 4000 and 600 cm⁻¹, with a Nicolet Magna 750 FTIR spectrometer equipped with a liquid N₂-cooled detector, a germanium-coated KBr beam splitter, and a globar source. One hundred interferograms were accumulated, and the resolution was also set to 0.12 cm⁻¹.

3. Computational Details

Minimum-energy structures of the four stereoisomers of formimidic acid, denoted (s-Z)-(E), (s-Z)-(Z), (s-E)-(Z), and (s-E)-(E), have been fully optimized at the B3LYP/6-311+G-(2d,2p) level of theory.[12,13] The first notation refers to the conformation of the molecule with respect to the C−O single bond and the second to that with respect to the C=N double bond. Normal coordinate calculations were carried out for each minimum; the resulting vibrational frequencies remained unscaled. All these calculations were performed with the GAUSSIAN 98 program.[14]
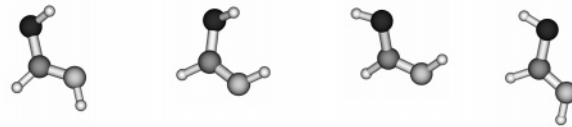
A second step of these calculations was the identification of the transition states involved in the reactional pathways describing the isomerizations between the four stereoisomers. For that, we performed first semiempirical calculations to localize the transition states (TS) and then to obtain the reaction pathways. After that we used the semiempirical geometries to perform ab initio optimization followed by ab initio TS calculations. We also used an IRC (internal reaction coordinate) procedure to check the reaction pathways and estimate the barrier heights.

The semiempirical calculations have been performed with the full-chain method included in the AMPAC package.

4. Results and Discussion

Theoretical Calculations. All the optimized geometrical parameters of the four stereoisomers, together with the energy differences compared to the most stable, that is, the (s-Z)-(E) stereoisomer, are gathered in Table 1. (s-Z)-(E) is the most stable form, while (s-Z)-(Z), (s-E)-(Z), and (s-E)-(E) have energetic differences of 15, 15.5, and 23 kJ mol⁻¹, respectively. These four stereoisomers will be hereafter noted **1**, **2**, **3**, and **4**, respectively. As for their geometrical parameters, it is worth noting that they all have very close planar structures. Concerning the higher stability of **1**, it is certainly due to the existence of an intramolecular bond between the hydroxylic H and the N atom, calculated with a distance of 2.3 Å. Our vibrational assignment is based on the comparison of the experimental and theoretical sets of bands. The harmonic frequencies are gathered in Table 2. Two spectral regions (OH and C=N stretching regions) are of particular interest in order to discriminate the vibrational spectra of each isomer.

Photodecomposition of Formimidic Acid

J. Phys. Chem. A, Vol. 109, No. 49, 2005 **11157**

TABLE 2: Theoretical Frequencies of the Four Isomers of Formimidic Acid[a]

Assignment	(s-Z)-(E): (1)	(s-Z)-(Z): (2)	(s-E)-(Z): (3)	(s-E)-(E): (4)	$\Delta\nu_{21}$	$\Delta\nu_{31}$	$\Delta\nu_{41}$
(OH)	3746 (18)	3784 (13)	3824 (18)	3851 (36)	38	78	105
(NH)	3536 (4)	3455 (3)	3470 (2)	3537 (6)			
(CH)	3113 (9)	3166 (3)	3116 (7)	3040 (24)			
C=N	1714 (100)	1715 (100)	1749 (64)	1746 (97)	1	35	32
CH/ NH	1396 (8)	1410 (0)	1418 (4)	1417 (7)			
CH/ NH/ OH	1371 (0)	1346 (12)	1303 (100)	1328 (77)			
CH/ OH/ NH	1192 (32)	1127 (82)	1175 (9)	1192 (20)			
NH+ CO	1062 (68)	1069 (28)	1056 (18)	1049 (100)			
OH/ NH	1045 (0)	1064 (22)	1056 (15)	1033 (0)			
NH	825 (12)	847 (18)	870 (8)	826 (30)			

[a] Relative intensities are given as percentages. $\Delta\nu_{i1} = \nu(\text{isomer } i) - \nu(\text{isomer 1})$: $\Delta\nu_{21}$, ν(s-Z)-(Z) $- \nu$(s-Z)-(E); $\Delta\nu_{31}$, ν(s-E)-(Z) $- \nu$(s-Z)-(E); $\Delta\nu_{41}$, ν(s-E)-(E) $- -\nu$(s-Z)-(E). ν, stretching; δ, bending; τ, torsion. Theoretical frequencies were obtained by use of B3LYP/6-311+G(2d,2p).

For example, the νOH mode of **1** is calculated at 3746 cm^{-1}, compared to 3784, 3824, and 3851 cm^{-1} for **2**, **3** and **4**, respectively, leading to respective shifts of 38, 78, and 105 cm^{-1} with respect to **1** (Table 2).

In the νC=N region we can separate the lower frequency stereoisomers **1** and **2**, predicted at 1714 and 1715 cm^{-1}, respectively, from the higher frequency **3** and **4**, predicted at 1749 and 1746 cm^{-1} respectively. As in the upper case, if we refer to **1**, the shifts are 1, 35, and 32 cm^{-1}. For **1** and **2**, the νC=N mode is the most intense, while the δNH and δOH modes are the most intense in the case of **3** and **4** (Table 2).

The second part of our theoretical investigations was devoted to the reactional pathways of the isomerization reactions and the localization of the transition states. Following the two-step procedure described under Computational Details, we have examined the reaction pathways involved in the isomerizations between the four stereoisomers. These reaction pathways are displayed in Figure 1.

In the case of the rotation around the single C−O bond, the transition state for the reaction between **1** and **4**, noted Ts1, is found to be 45 kJ mol^{-1} (ca. 3700 cm^{-1}) above **1**. The transition state (Ts2) of the reaction between **2** and **3** is found to be 35 kJ mol^{-1} (ca. 3000 cm^{-1}) above **2**. These two transition-state structures are found to be nonplanar, exhibiting HCOH dihedral angles close to 90°. These two barrier heights are typical of IR energies. Thus we expect to be able to induce these reactions by irradiating in the νOH spectral region.

In the case of rotation around the C=N double bond, that is, **1** → **2** and **3** → **4**, the barrier heights are predicted to be in both cases about 100 kJ mol^{-1} (i.e., 9000 cm^{-1}). The two transition states, respectively Ts3 and Ts4, display planar structures with CNH angles of 180° (Figure 1). The experimental implication is that it should be impossible to induce these isomerizations by irradiating in the νOH spectral region. Finally, we specify that we did not perform any reaction pathway calculations for the formamide → formimidic acid reactions because it has already been done by Maier and Endres[3] in the S0 electronic state and will be the subject of a forthcoming publication.

FTIR Spectra of Formimidic Acid in Xe, N₂, Ar, and Ne Matrices. After 500 min of irradiation at 240 nm in Xe, N₂, Ar, and Ne, the formamide absorption bands nearly vanish while new absorptions due to formimidic acid grow (Figure 2). Besides the bands related to the formimidic acid, we also observe several other products yielded in a small amount such as the CO·NH₃ and the HNCO·H₂ complexes. These products have been already reported by Lundell et al.[2] in their formamide decomposition study performed at 193 nm. In addition, we also observe after formamide irradiation in argon matrix a small band at 3608 cm^{-1} (Figure 2) whose origin will be further discussed below in the text.

As shown in Figure 2, which displays the ν(OH) and ν(C=N) stretching regions of formimidic acid, several bands are observed in each region that suggest the presence of several photoproducts. From comparisons between experimental and theoretical frequency shifts in these two regions (labeled in Table 3 as $\Delta\nu_{i1} = \nu(\text{isomer } i) - \nu(\text{isomer 1})$, we deduce that two different structures of formimidic acid are found in Xe (Figure 2a), Ne (Figure 2d), and Ar (Figure 2c), whereas three different isomers are detected in N₂ matrix (Figure 2b).

In the ν(OH) region, the most intense band observed in Xe, N₂, Ar and Ne matrices is located at 3529, 3550, 3557, and 3570 cm^{-1}, respectively. This band corresponds to the most stable structure, **1**, which is expected from the theoretical calculations to give the lower frequency in the ν(OH) region. Such a shift for a ν(OH) mode relative to the same species is consistent with a matrix effect [ν(Xe) < ν(N₂) < ν(Ar) < ν(Ne)], which is generally observed in the matrix isolation studies.[15−17] We notice also that the frequency of this mode is lower than the free OH stretching mode expected above 3600 cm^{-1} in argon matrix and this change is mainly due to an intramolecular hydrogen bond as shown in the previous part.

In Ar and Ne matrices (Figure 2c,d), in addition to the absorption bands assigned to the most stable stereoisomer, we observe weaker bands located at 3592 and 3609 cm^{-1} in each respective matrix. The shifts of these bands are 35 and 39 cm^{-1} toward the higher wavenumbers in comparison with the **1**
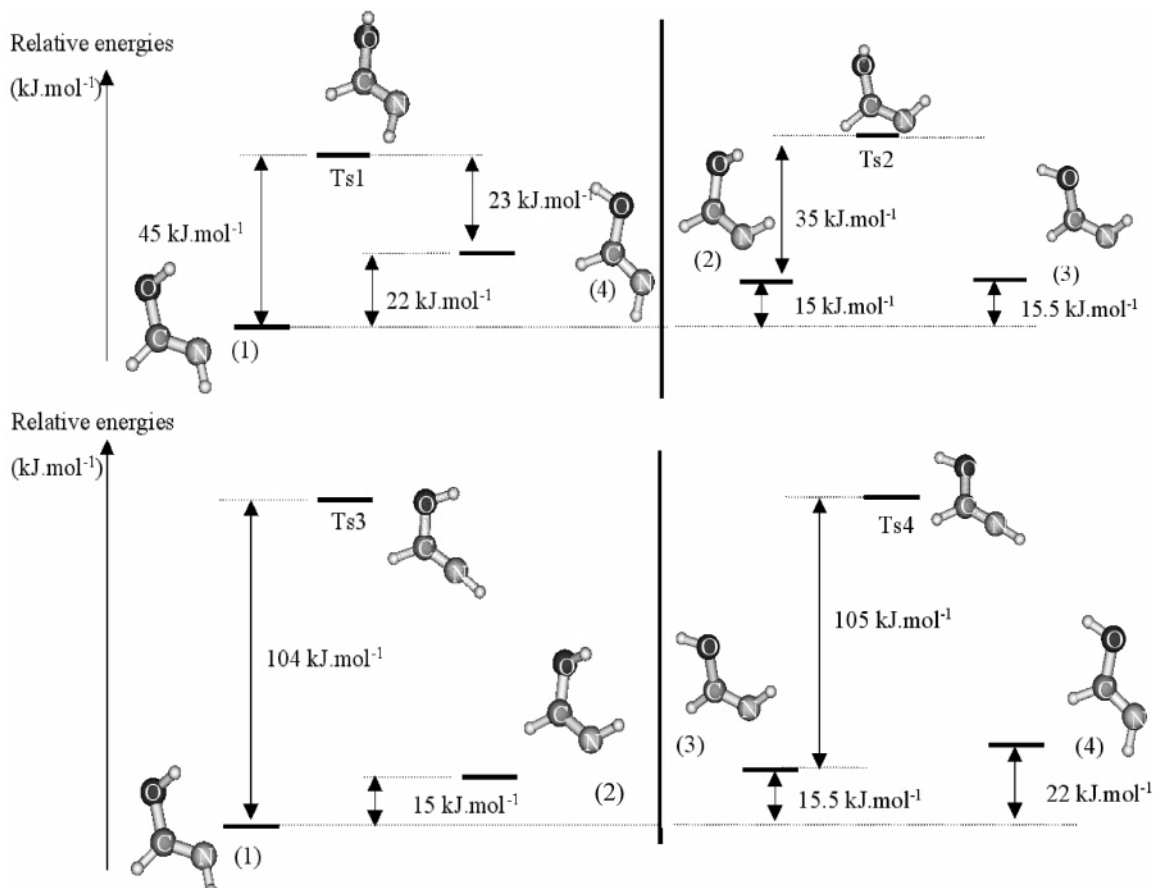
Figure 1. Theoretical isomerization pathways between the four conformers of formimidic acid. Stationary points and transition states were performed with the B3LYP/6-311+G(2d,2p) method.
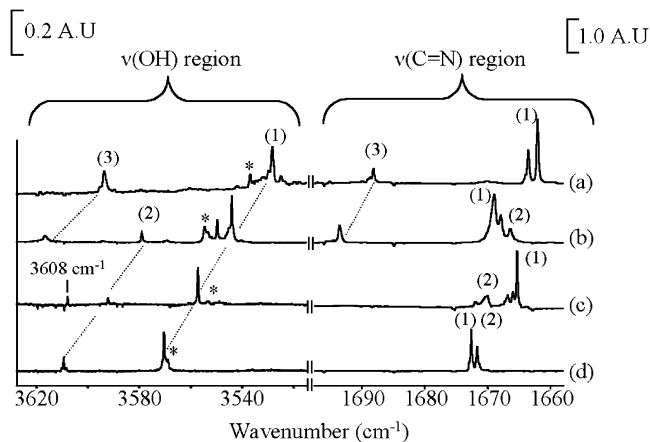
Figure 2. FTIR spectra of formimidic acid at 4 K obtained from formamide irradiated with wavelength of 240 nm (500 min) in (a) xenon matrix, (b) nitrogen matrix, (c) argon matrix, and (d) neon matrix. Asterisks indicate $\nu(NH_2)$ stretching mode of remaining formamide. Labels for isomers **1**−**4** of formimidic acid (see text) are shown in parentheses. AU, absorbance unit.

TABLE 3: Comparison between Experimental and Theoretical Frequency Shifts[a]

| | | exptl frequencies/ exptl shifts $\Delta\nu_{i1}$(exp) (cm^{-1}) | | | theor shifts[b] | |
	Xe	N$_2$	Ar	Ne	$\Delta\nu_{i1}$(theo)	species
			ν_i(OH)			
ν_1	3529	3550	3557	3570		(s-Z)-(E)
$\nu_2/\Delta\nu_{21}$		3580/30	3592/35	3609/39	38	(s-Z)-(Z)
$\nu_3/\Delta\nu_{31}$	3593/64	3617/67			78	(s-E)-(Z)
$\nu_4/\Delta\nu_{41}$		3632/82			105	(s-E)-(E)
			ν_i(CN)			
ν_1	1662	1669	1665	1672		(s-Z)-(E)
$\nu_2/\Delta\nu_{21}$		1666/−3	1670/5	1673/1	1	(s-Z)-(Z)
$\nu_3/\Delta\nu_{31}$	1688/26	1694/25			35	(s-E)-(Z)
$\nu_4/\Delta\nu_{41}$		1690/21			32	(s-E)-(E)

[a] $\Delta\nu_{i1} = \nu$(isomer i) − ν(isomer 1) for the ν(OH) and ν(C=N) modes. [b] Theoretical shifts were obtained by use of B3LYP/6-311+G(2d,2p).

frequency observed in these two matrices. These values are in good agreement with the computational values reported above (38 cm^{-1}) for **2** (Table 3).

In Xe matrix, besides the band at 3529 cm^{-1} assigned to the **1** tautomer, we also observe a weaker band located at 3593 cm^{-1}, shifted by 64 cm^{-1} with respect to the first band. This shift is close to the predicted value (78 cm^{-1}) calculated between **1** and **3** stereoisomers. Thus the band at 3593 cm^{-1} is assigned to isomer **3**.

In N$_2$ matrix, we observe in the ν(OH) region two weak absorption bands located at 3580 and 3617 cm^{-1}, which are shifted by 30 and 67 cm^{-1} with respect to the frequencies of the **1** tautomer. As above, these shift values are consistent with the presence of **2** and **3** structures in this matrix. The case of the band located at 3554 cm^{-1} remains unclear because no comparison between the theoretical and experimental shifts seems possible. As will be confirmed below, we assign this band to a site trapping.

In the ν(C=N) region (1700−1665 cm^{-1}) we observe, as was predicted by quantum calculation, new vibrational bands, which grow in two different ranges: a "low frequency" range (1662−

Photodecomposition of Formimidic Acid

J. Phys. Chem. A, Vol. 109, No. 49, 2005 **11159**
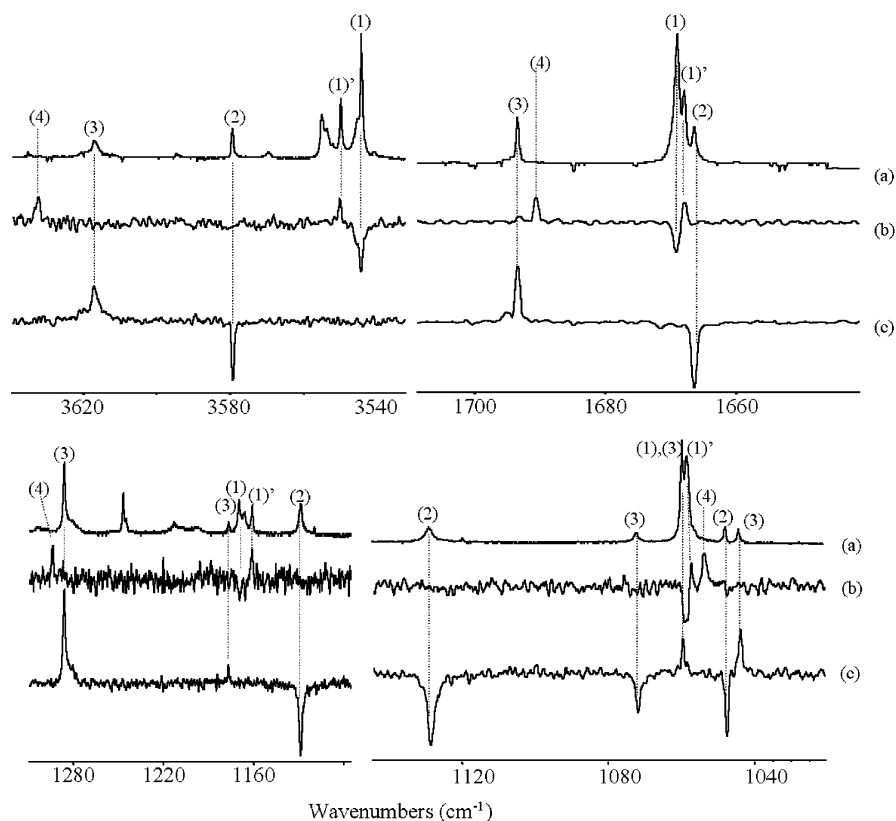
Figure 3. FTIR spectra of formimidic acid in nitrogen matrix at 4 K before infrared irradiation (a) and difference spectra showing the effect of selective IR irradiation on the ν(OH) stretching mode of isomer **1** at 3544 cm^{-1} (b) and isomer **2** at 3580 cm^{-1} (c). Labels for isomers **1**−**4** of formimidic acid are shown in parentheses. **1′** is the trapping site of isomer **1**.

TABLE 4: Comparison of Calculated Frequencies for the (s-Z)-(E) Stereoisomer of Formimidic Acid (1) with Experimental Frequencies[a]

	exptl frequencies (cm^{-1})				calcd frequencies (cm^{-1})
assignment	Xe	N$_2$	Ar	Ne	
νOH	3529 (m)	3544−3550 (m)	3557 (m)	3570 (m)	3746 (18)
νNH	3381 (w)	3362 (w)		3381 (w)	3536 (4)
νCH	2971 (w)	2980 (w)	2988 (w)	2971 (w)	3113 (9)
νC=N	1662 (s)	1669−1667 (s)	1665 (s)	1672 (s)	1714 (100)
δCH/δNH	1365 (m)	1372 (m)	1367 (m)	1365 (w)	1396 (8)
δCH/δNH/δOH					1371 (0)
δCH/δOH/δNH	1170 (m)	1166 (m)	1169 (m)	1170 (m)	1192 (32)
δNH + νCO	1046 (m)	1058 (m)	1045 (m)	1046 (m)	1062 (68)
τOH/τNH					1045 (0)
τNH		817 (w) 828−832 (w)	816 (w)	817 (w)	825 (12)

[a] Calculated frequencies were obtained by use of B3LYP/6-311+G(2d,2p). Experimental frequencies were obtained after irradiation of formamide at λ = 240 nm at 4 K in Xe, N$_2$, Ar, and Ne matrices. Theoretical relative intensities are given in parentheses and are normalized to the most intense band. Experimental relative intensities are indicated by s, strong; m, medium; and w, weak. ν, stretching; δ, bending; τ, torsion.

1672 cm^{-1}) linked with **1** and **2** (Figure 2) and a "high frequency" range (1688−1694 cm^{-1}) linked to conformers **3** and **4** (Figure 2). The experimental shift close to 25 cm^{-1} between these two frequency groups is consistent with the value predicted by the calculations (35 cm^{-1}). The large number of features observed in the lower frequency area: two in Xe (Figure 2a), three in N$_2$ (Figure 2b), four in argon (Figure 2c), and two in Ne (Figure 2d) suggests that the structure **1** is trapped in different sites in Xe, N$_2$, and Ar matrices. The weakest bands observed at 1666 cm^{-1} in N$_2$, 1670 cm^{-1} in Ar and 1671 cm^{-1} in Ne are due to the structure **2**. The structure **3** is observed exclusively in Xe at 1688 cm^{-1} and in N$_2$ at 1694 cm^{-1}. The

observation of this latter structure is supported by the presence of strong bands located at 1300 and 1286 cm^{-1} in Xe and N$_2$ matrices, respectively. Moreover, due to the fact that these latter bands are the most intense of the observed spectra, we assign them to the δ(OH) bending mode of **3**, as predicted by the theoretical results.

At this point of the study, we observe in argon and neon matrices that the irradiation of formamide leads to the formation of structures **1** and **2**. In xenon matrix, it leads to the formation of the **1** and **3** structures, while we observed the formation of the three structures **1**, **2** and **3** in nitrogen matrix. These results confirm those reported by Maier and Endres,[3] who have observed in argon matrix the presence of only stereoisomers **1** and **2**. The correlated changes of isomer distribution with the rare gas matrices cannot be explained only by the isomer stability. Indeed, the **2** and **3** isomers are predicted to have similar energies and thus these two forms should be similarly populated. The matrix cage sizes and thus the steric effect do not seem to have a striking impact on isomer stabilization. Indeed, in Xe, which has the largest cage size matrix, we do not observe the three forms. Then it seems that the changes in the distribution of stereoisomers according to rare gas matrices are induced by the polarizability of the matrix.[15] For example, **3**, for which the OH group is s-trans with respect to the C=N bond and which has a calculated dipolar moment (2.8 D) higher than that of **2** (2 D), is not observed in low-polarizability Ar and Ne matrices.[18] On the contrary, this structure is observed in Xe, which is known to be the most polarizable matrix.[18] Concerning the stereoisomer of weakest polarity, **2**, we observe it only in low-polarizability matrices such as Ar and Ne and not in Xe.

On the other hand, it has been reported that the N$_2$ matrix has a polarizability on the order of Ar.[18] Despite this fact, the

TABLE 5: Comparison of Calculated Frequencies for the (s-Z)-(Z) Conformer of Formimidic Acid (2) with Experimental Frequencies[a]

	exptl frequencies (cm^{-1})			calcd frequencies (cm^{-1})
assignment	N$_2$	Ar	Ne	
νOH	3580 (w)	3592 (w)	3609 (w)	3784 (13)
νNH	3357 (w)			3455 (3)
νCH		3055 (w)	3048 (w)	3166 (3)
νC=N	1666 (s)	1670 (s)	1671 (s)	1715 (100)
δCH/δNH				1410 (0)
δCH/δNH/δOH	1332 (w)	1335 (w)	1337−1332 (w)	1346 (12)
δCH/δOH/δNH	1128 (m)	1099 (m)	1099 (m)	1127 (82)
δNH + νCO	1073 (m)	1053 (m)	1053 (m)	1069 (28)
τOH/τNH	1048 (m)	1048 (m)	1041 (m)	1064 (22)
τNH	841 (w)	832 (w)	833 (w)	847 (18)

[a] Calculated frequencies were obtained by use of B3LYP/6-311+G(2d,2p). Experimental frequencies were obtained after irradiation of formamide at λ = 240 nm at 4 K in N$_2$, Ar, and Ne matrices. Theoretical relative intensities are given in parentheses and are normalized to the most intense band. Experimental relative intensities are indicated by s, strong; m, medium; and w, weak. ν, stretching; δ, bending; τ, torsion.

TABLE 6: Comparison of Calculated Frequencies for the (s-E)-(Z) Conformer of Formimidic Acid (3) with Experimental Frequencies[a]

	exptl frequencies (cm^{-1})		calcd frequencies (cm^{-1})
assignment	Xe	N$_2$	
νOH	3593 (w)	3617 (w)	3824 (18)
νNH			3470 (2)
νCH		3299 (w)	3116 (7)
νC=N	1688 (s)	1694 (s)	1748 (64)
δCH/δNH		1391 (w)	1418 (4)
δCH/δNH/δOH	1300 (s)	1286 (s)	1303 (100)
δCH/δOH/δNH	1166−1167 (w)	1177 (w)	1175 (9)
δNH + νCO		1058 (w)	1056 (18)
τOH/τNH		1043 (w)	1056 (15)
τNH	847 (w)	860 (w)	870 (8)

[a] Calculated frequencies were obtained by use of B3LYP/6-311+G(2d,2p). Experimental frequencies were obtained after irradiation of formamide at λ = 240 nm at 4 K in Xe and N$_2$ matrices. Theoretical relative intensities are given in parentheses and are normalized to the most intense band. Experimental relative intensities are indicated by s, strong; m, medium; and w, weak. ν, stretching; δ, bending; τ, torsion.

three structures pointed out above are detected. It seems that the stabilization of the isomers is ruled by the electrostatic interaction between their OH groups and the N$_2$ molecules of the cryogenic crystal instead of the polarizability of the matrix.[19]

IR Excitation of Formimidic Acid Stereoisomers. As reported in the literature, infrared irradiation is able to induce changes in the conformational distribution of a molecule in a low-temperature matrix.[20−24] The mechanism that is generally proposed to explain the isomerization processes involves absorption of radiation, followed by a conversion into internal rotation modes by intramolecular energy transfer only if the internal rotation barrier is on the order of the energy of the IR photon. In our case, from our theoretical calculations, an IR irradiation in the ν(OH) region at ca. 3600 cm^{-1} (i.e., 43 kJ·mol^{-1}) should provide sufficient energy to overcome the rotation barrier around the C−O bond. Then, all isomers of the formimidic acid could be observed and the assignment of the vibrational bands of each isomer should be realized unequivocally.

We will just describe below the selective IR irradiations that we performed in N$_2$ matrix because this is the only matrix in which we have observed striking effects. Indeed, when the same

TABLE 7: Comparison of Calculated Frequencies for the (s-E)-(E) Conformer of Formimidic Acid (4) with Experimental Frequencies[a]

assignment	N$_2$	calcd frequencies (cm^{-1})
ν(OH)	3632 (w)	3851 (36)
ν(NH)		3537 (6)
ν(CH)		3040 (24)
ν(C=N)	1690 (s)	1746 (97)
δ(CH/δNH)		1417 (7)
δCH/δNH/δOH	1293 (s)	1328 (77)
δCH/δOH/δNH		1192 (20)
δNH + νCO	1053 (s)	1049 (100)
τOH/τNH		1033 (0)
τ NH		826 (30)

[a] Calculated frequencies were obtained by use of B3LYP/6-311+G(2d,2p). Experimental frequencies were obtained after IR irradiation (3544 cm^{-1}) of the (s-Z)-(E) isomer of formimidic acid at 4 K in an N$_2$ matrix Theoretical relative intensities are given in parentheses and are normalized to the most intense band. Experimental relative intensities are indicated by s, strong; m, medium; and w, weak. ν, stretching; δ, bending; τ, torsion.

irradiations were carried out in the three other matrices, no noticeable spectral changes were observed at our recording time scale, that is, 30 s for each spectrum. It does not mean that no photoeffects occur, but certainly that our recording time scale is too long compared to the lifetime of the photoproducts in these three media.[25,26]

Irradiation at 3544 cm^{-1}. The main effect of irradiation at 3544 cm^{-1} of the ν(OH) mode of stereoisomer **1** is the decrease of the bands at 3544, 3362, 2980, 1669, 1058, and 828 cm^{-1} counterbalanced by the increase of those at 3550, 1667, 1057, and 832 cm^{-1} on one hand and on the other hand by the appearance of those at 3632, 1690, 1293, and 1053 cm^{-1} (Figure 3b, Table 4). If we compare the experimental sets of bands with the theoretical ones, it is clear that the former set of increasing bands is due to a trapping site of the stereoisomer **1**, labeled **1'**, whereas the second set matches isomer **4** (Table 3). Thus the IR irradiation of the ν(OH) stretching mode of **1** leads to isomer **4**. It should be noted that we observe a complete back reaction from **4** to **1** in 10 min at 4.4 K in the IR beam of the spectrophotometer. We think that the globar photons are mainly involved in this back reaction.

Irradiation at 3580 cm^{-1}. After the irradiation on the ν(OH) mode of stereoisomer **2** at 3580 cm^{-1} (Figure 3c), we observe the decrease of bands centered at 3580, 3357, 1666, 1332, 1128, 1073, 1048, and 841 cm^{-1}, while those assigned to **3** at 3617, 3299, 1694, 1391, 1286, 1177, 1058, 1043, and 860 cm^{-1} increase. Irradiation at 3617 cm^{-1} allows the complete back isomerization of **3** to **2**. It is also obvious that the globar photons induce also this back conversion but at a lower rate.

These IR-selective irradiations allowed us to suggest a complete vibrational assignment for each stereoisomer and they have been used to compare the sets of vibrational bands in the three other matrices (Tables 4−7).

UV Irradiation (λ > 160 nm) of Formimidic Acid. The vacuum UV irradiations (λ > 160 nm) of formimidic acid were performed in Ar and Xe matrices at 10 K. The half-life of formimidic acid decomposition in Ar matrix is reached after 260 min, whereas in xenon matrix, it is reached after only 15 min.

Thus, after vacuum UV irradiation in Ar and Xe matrices of formimidic acid, new bands appear, particularly in the typical region of isocyanic acid (HNCO),[27] HCN (2100−2090 cm^{-1}),[28] HNC (2060−2040 cm^{-1}),[29] and also in the typical region of water (3700−3600 and 1650−1500 cm^{-1}) (Figure 4, Table 8).[30]

Photodecomposition of Formimidic Acid

J. Phys. Chem. A, Vol. 109, No. 49, 2005 **11161**
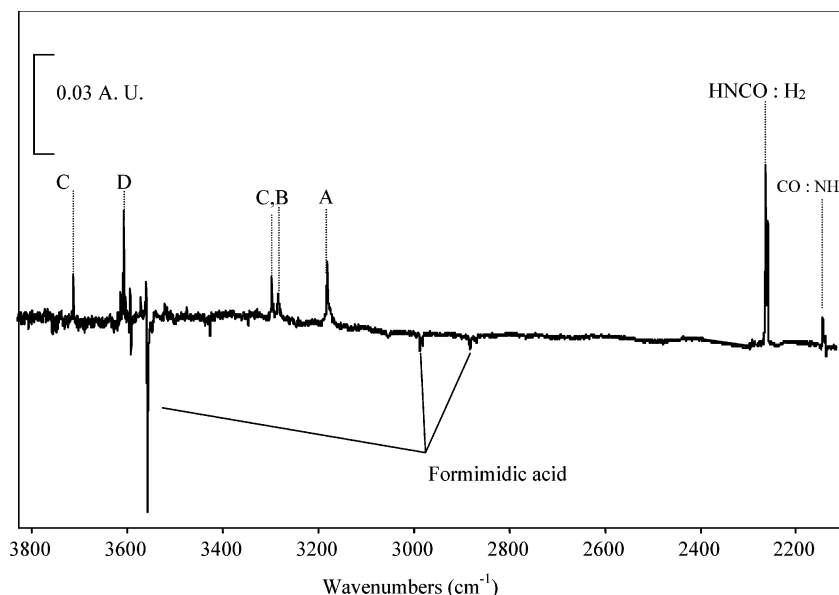
Figure 4. FTIR difference spectrum between the formimidic acid in argon matrix before irradiation and after vacuum UV irradiation (500 min) at $\lambda > 160$ nm in argon matrix at 10 K; the products arising from the photodissociation process are shown as positive, and the formimidic acid appears as negative. AU, absorbance unit.

SCHEME 2: Possible Mechanism of Decomposition of Formimidic Acid
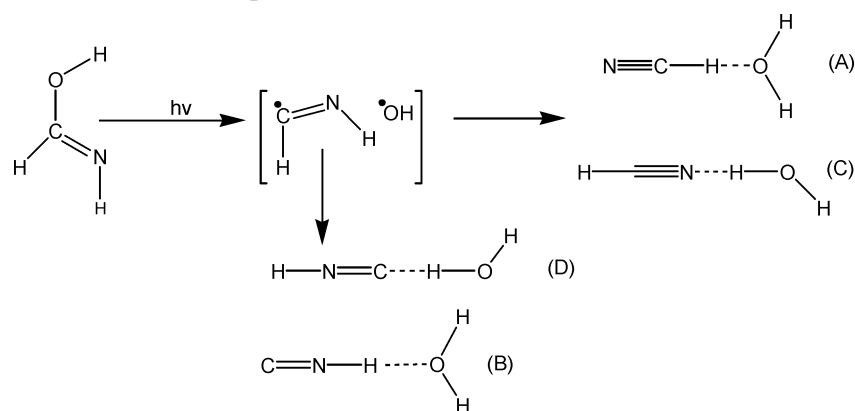
By comparison with previous studies, we can easily assign each of these bands to different complexes. The formation of the HNCO·H_2 complex after vacuum UV irradiation of formimidic acid is deduced from the presence of its strong bands located at 2264 cm^{-1} in argon matrix or 3480 and 2254 cm^{-1} in xenon matrix.[2] The HNCO·H_2 complex (Figure 4, Table 8) has been already observed by Lundell et al.[2] in their photodecomposition study of formamide at 193 nm in argon and xenon matrices. Thus, formimidic acid is also a source of the HNCO·H_2 complex. We suggest that the reaction pathway leading to this complex from formimidic acid involves a cleavage of the OH and CH bonds followed by recombination of hydrogen atoms. In addition, in the νCO stretching region, we observe after irradiation a small band at 2145 cm^{-1} in argon matrix due to the CO·NH complex coming from HNCO photolysis.[31]

After 505 min of irradiation of the formimidic acid ($\lambda > 160$ nm), we observe the formation in argon matrix of two different hydrogen-bonded HCN·H_2O and HNC·H_2O complexes displaying two orientations: NCH−OH_2 (complex A) and HCN−HOH (complex B) for the first type of complex and CNH−OH_2 (complex C) and HNC−HOH (complex D) for the second type (Figure 4). The structures of these complexes are shown in Scheme 2. The identification of these complexes is based on a recent study in which Heikkilä et al.[32] report the vibrational bands of these complexes from the irradiation in argon matrix

of the formaldoxime (H_2C=NOH), an isomer of formimidic acid. The bands assigned in our spectra to these complexes are labeled in Figure 4 and the frequencies are reported in Table 8. It is noticeable that before the formimidic acid irradiation at 160 nm (i.e., after the photolysis of formamide at 240 nm in order to form formimidic acid), a small amount of complex A is observed, characterized by the band located at 3608 cm^{-1} (Figure 2). Thus we can conclude that formimidic acid is also able to be dissociated at 240 nm. Nevertheless, at this wavelength, the photoprocess is less efficient than at 160 nm, which suggests that the formimidic acid could have an absorption band closer to 160 nm than 240 nm.

Using the results in argon matrix, we also observe in xenon matrix that a sharp band in the ν(CN) region at 2088 cm^{-1} grows after irradiation of the formimidic acid, which can be assigned to complex A (Table 8). In the ν(CH) and ν(NH) stretching region, two bands at 3290 and 3284 cm^{-1} can be assigned to complexes B and C, respectively (Table 8). Unfortunately, with our experimental conditions in xenon matrix, we did not detect complex D. As for the formaldoxime, the formation of these complexes should result from a breaking of the CO bond and formation of the OH radical, followed by a recombination of this radical with one of the hydrogen atoms of HCNH radical to yield either HNC + H_2O or HCN + H_2O (see Scheme 2). This dehydration process has been considered only from a

TABLE 8: Observed Absorption Bands after Vacuum UV-Induced Photodecomposition of Formimidic Acid in Argon and Xenon Matrices at 10 K

obs band (cm^{-1})				
argon	xenon	species	complex[a]	assignment[b]
3715		H$_2$O (+HCN)	C	ν(OH)
3608		HNC (+H$_2$O)	D	ν(NH)
3594		H$_2$O (+HCN)	C	ν(OH)
3560		H$_2$O (+HNC)	D	ν(OH)
	3480	HNCO (+H$_2$)		ν(NH)
	3439	?		
3298	3290	HCN (+H$_2$O)	C	ν(CH)
3284	3284	HNC (+H$_2$O)	B	ν(NH)
3184	3130	HCN (+H$_2$O)	A	ν(CH)
2264	2254	HNCO (+H$_2$)		ν(NCO)
2145		CO (+NH)		ν(CO)
2090	2088	HCN (+H$_2$O)	A	ν(CN)
2048		HNC (+H$_2$O)	D	ν(CN)
1629		H$_2$O (+HCN)	C	δ(HOH)
1598		H$_2$O (+HCN)	A	δ(HOH)
	843	HCN (+H$_2$O)	A	δ(HCN) oop
766	763	?		
727	729	HCN (+H$_2$O)	C	δ(HCN) oop

[a] (A) NCH·OH$_2$ complex; (B) CNH·OH$_2$ complex; (C) HCN·HOH complex; (D) HNC·HOH complex. [b] ν, stretching; δ, bending; oop, out of plane.

theoretical point of view in the case of acetamide, and the most favorable mechanism leading to the dehydration product is described as occurring in the ground state.[33]

5. Conclusion

UV irradiation at 240 nm of formamide induces mainly a conversion of this molecule into formimidic acid, resulting in an 1,3 intermolecular hydrogen transfer. According to the matrix gas, two or three different species are observed after irradiation, and it seems that the polarizability of the matrix has an effect on this selectivity. The most intense bands are assigned to the most stable structure **1** predicted by ab initio calculations. From infrared-induced isomerization experiments performed in N$_2$ matrix, exciting the ν(OH) stretching mode of each stereoisomer, conversions between conformers occur: **1**→**4** and **2**→**3**. An accurate assignment of the bands of each of these species has been realized.

The broad-band UV irradiation of formimidic acid performed at λ > 160 nm leads to two main processes, dehydrogenation and dehydration. In the first case, HNCO·H$_2$ complex is formed, whereas in the second case, HNC and HCN in interaction with water are yielded. The dehydration reaction concerning amides

or their tautomers is reported for the first time, and that can induce new insight into the photochemical mechanism of these molecules.

References and Notes

(1) Schlegel, H.; Gund, P.; Fluder, M. *J. Am. Chem. Soc.* **1982**, *104*, 5347.
(2) Lundell, J.; Krajewska, M.; Räsänen, M. *J. Phys. Chem. A* **1998**, *102*, 6643.
(3) Maier, G.; Endres, J. *Eur. J. Org. Chem.* **2000**, 1061.
(4) Duvernay, F.; Chiavassa, T.; Borget, F.; Aycard, J. P. *J. Phys. Chem. A* **2005**, *109*, 6008.
(5) Rostkowska, H.; Lapinski, L.; Khvorostov, A.; Nowak, M. *J. Phys. Chem. A* **2003**, *107*, 6373.
(6) Nowak, M.; Lapinski, L.; Rostkowska, H.; Les, A.; Adamowicz, L. *J. Phys. Chem.* **1991**, *94*, 7406.
(7) Nowak, M.; Lapinski, L.; Fulara, J.; Les, A.; Adamowicz, L. *J. Phys. Chem.* **1991**, *95*, 2404.
(8) Wang, X.; Nichols, J.; Feyereisen, M.; Gutowski, M.; Boatz, J.; Haymet, A.; Simons, J. *J. Phys. Chem.* **1991**, *95*, 10419.
(9) Bash, H.; Robin, M.; Kuebler, N. *J. Chem. Phys.* **1968**, *49*, 5007.
(10) Ballard, R.; Jones, J.; Read, D.; Inchley, A.; Cranmer, M. *Chem. Phys.* **1988**, *147*, 629.
(11) Gingell, J.; Mason, N.; Zhao, H.; Walker, I.; Siggel, M. *Chem. Phys.* **1997**, *220*, 191.
(12) Lee, C.; Yang, W.; Parr, R. *Phys. Rev. B* **1988**, *37*, 785.
(13) Becke, A. D. *Phys. Rev. A* **1988**, *38*, 3098.
(14) Frisch, M., et al. GAUSSIAN 98, Revision A.7; Gaussian Inc.: Pittsburgh, PA, 1998.
(15) Barnes, A. J. *J. Mol. Struct.* **1984**, *113*, 161.
(16) Chiavassa, T.; Verlaque, P.; Pizzala, L.; Allouche, A.; Roubin, P. *J. Phys. Chem.* **1993**, *97*, 5917.
(17) Aspiala, A.; Murto, J.; Pekka, S. *Chem. Phys.* **1986**, *106*, 399.
(18) Hallam, H. E. *Vibrational Spectroscopy of Trapped Species*; Wiley: London, 1973.
(19) Murto, J.; Ovaska, M. *Spectrochim. Acta, Part A* **1983**, *39*, 149.
(20) Baldeschwieler, J. D.; Pimentel, G. C. *J. Chem. Phys.* **1960**, *33*, 1008.
(21) Hall, R. T.; Pimentel, G. C. *J. Chem. Phys.* **1963**, *38*, 1889.
(22) Coussan, S.; Manca, C.; Ferro, Y.; Roubin, P. *Chem. Phys. Lett.* **2003**, *370*, 118
(23) Aspiala, A.; Lotta, T.; Murto, J.; Räsänen, M. *J. Chem. Phys.* **1983**, *79*, 4183.
(24) Pourcin, J.; Davidovics, G.; Bodot, H.; Abouaf-Marguin, L.; Gauthier-Roy, B. *Chem. Phys. Lett.* **1980**, *74*, 147.
(25) Lotta, T.; Murto, J.; Räsänen, M.; Aspiala, A.; Särkkä, P. *J. Chem. Phys.* **1985**, *82*, 1363.
(26) Räsänen, M.; Aspiala, A.; Murto, J. *J. Chem. Phys.* **1983**, *79*, 107.
(27) Teles, J. H.; Maier, G.; Hess, B. A.; Schaad, L. J.; Winnewisser, M.; Winnewisser, B. P. *Chem. Ber.* **1989**, *122*, 753.
(28) Abbate, A.; Moore, C. *J. Chem. Phys.* **1985**, *82*, 1255.
(29) Milligan, D. E.; Jacox, M. E. *J. Chem. Phys.* **1967**, *47*, 278.
(30) Ayers, G.; Pulling, D. *Spectrochim. Acta* **1976**, *32A*, 1629.
(31) Petterson, M.; Kriachtchev, L.; Jolkkonen, S.; Räsänen, M. *J. Phys. Chem. A* **1999**, *103*, 9154.
(32) Heikkilä, A.; Pettersson, M.; Lundell, J.; Kriachtchev, L.; Räsänen, M. *J. Phys. Chem. A* **1999**, *103*, 2945.
(33) Chen, X. B.; Fang, W. H.; Fang, D. C. *J. Am. Chem. Soc.* **2003**, *125*, 9689.